Structural Engineering and Mechanics, *Vol. 58, No. 2 (2016) 217-230*
DOI: http://dx.doi.org/10.12989/sem.2016.58.2.217

Effects of temperature dependent material properties on mixed mode crack tip parameters of functionally graded materials

Mohammad Rajabi*, Nasser Soltani[a] and Iman Eshraghi[b]

Department of Mechanical Engineering, Intelligence Based Experimental Mechanics Center, University of Tehran, Tehran, Iran

(Received October 15, 2015, Revised December 27, 2015, Accepted December 27, 2015)

Abstract. Effects of temperature dependent material properties on mixed mode fracture parameters of functionally graded materials subjected to thermal loading are investigated. A domain form of the J_k-integral method including temperature-dependent material properties and its numerical implementation using finite element analysis is presented. Temperature and displacement fields are calculated using finite element analysis and are used to compute mixed mode stress intensity factors using the J_k-integral. Numerical results indicate that temperature-dependency of material properties has considerable effect on the mixed-mode stress intensity factors of cracked functionally graded structures.

Keywords: temperature dependent material properties; functionally graded materials; stress intensity factors; thermal gradient

1. Introduction

Functionally graded materials (FGMs) are inhomogeneous materials, in which material properties vary smoothly in one (or more) spatial direction(s). The concept of FGMs arose from the early attempts to meet stringent material requirements pertaining to aerospace vehicles facing thermal cycles between elevated and cryogenic temperatures (Koizumi 1997). The gradual variation in material properties has been shown to improve failure performance, while preserving the intended thermal, tribological and structural benefits of combining materials (Birman and Byrd 2007). In recent years, FGMs received increasing research interests in the scientific community of different disciplines, because of their improved mechanical and thermal performances over the conventional composites (Ootao and Ishihara 2013, Abolbashari and Nazari 2014).

The operation of structures made from FGMs under thermal and mechanical loading conditions may trigger the initiation of micro-cracks which may expose the structural integrity into danger. Thus for safe operation of structures made from FGMs, it is essential that fracture behavior of them be well understood. Fracture of in-homogeneous materials has been a topic of research for many years (Atkinson and List 1978, Delale and Erdogan 1983). Usually Fracture problems in

*Corresponding author, Ph.D. Candidate, E-mail: mohammad.rajabi@ut.ac.ir
[a]Professor, E-mail: nsoltani@ut.ac.ir
[b]Ph.D. Candidate, E-mail: ieshraghi@ut.ac.ir

http://www.techno-press.org/?journal=sem&subpage=8 ISSN: 1225-4568 (Print), 1598-6217 (Online)

functionally graded materials are solved by specifying a functional form of material variation with spatial position, such as a linear or exponential profile (Guo and Noda 2007).

Both analytical and numerical approaches have been adopted by researches to analyze fracture of functionally graded materials (Gu *et al*. 1999, Petrova and Sadowski 2014, Bhardwaj *et al*. 2015, Eshraghi and Soltani 2015, Yu and Kitamura 2015). Among these approaches energy-based methods have received considerable attention since energy integrals can be easily calculated using the finite element results. Line integral around a vanishing contour at the crack tip was modified to a domain form to compute field quantities in a far-field region of the crack. In this way interaction integrals and J_k-integrals were two famous approaches taken by different researches to compute stress intensity factors. The former approach was utilized mainly by Paulino and his colleagues to analyze isotropic and orthotropic FGMs under both thermal and mechanical loadings (Kim and Paulino 2002), while the latter was primarily used by Dag (2007).

In most of the previously mentioned works mechanical and thermal properties of the FGM were taken as constant with respect to temperature. However as pointed out by Noda (1991), temperature-dependency of materials has considerable effect on the stress field and mechanical behavior of FGMs. Some researchers have considered the temperature-dependency of material properties in FGMs when used in extremely high or low temperature environments (Sumi and Sugano 1997, Reddy 2000). The aim of the current study is to investigate the effect of temperature-dependent material properties on the thermal fracture of functionally graded materials. To this end J_k-integral approach is used in its domain form where the temperature dependent material properties are taken into account for the computation of various terms of the integral. Numerical results are provided to investigate the effect of temperature dependency of material properties on mixed mode thermal stress intensity factors in a cracked functionally graded material.

2. Formulation

2.1 J_k-integral

J_k-integral is a line integral on a vanishingly small curve around the crack tip. Stress intensity factor values can easily be computed once the components of this energy integral are evaluated.

As shown in Fig. 1 a small contour around crack tip in a functionally graded material is

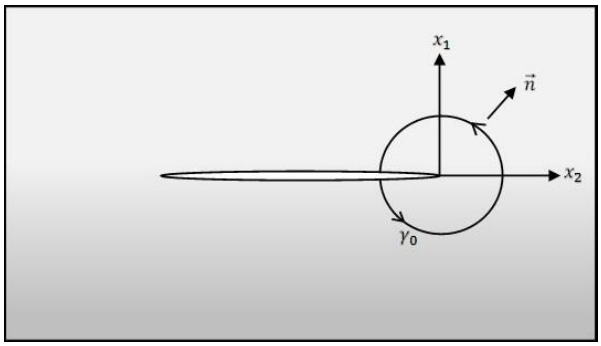

Fig. 1 A curve around crack tip in functionally graded material

considered. The J_k-integral may be defined as (Dag 2007)

$$J_k = \int_{\gamma_0 \to 0} (W n_k - \sigma_{ij} n_j u_{i,k}) ds \tag{1}$$

Where i, j, k=1, 2, W represents the internal strain energy density, n_k is the components of the normal vector to the curve γ_0, σ_{ij} is the stress components and u_i denotes the displacement components. Plane stress/strain conditions are assumed in Eq. (1) and $u_{.,k}$ represents differentiation with respect to k^{th} coordinate. It should be noted that J_1 represents the energy release rate (J-integral) introduced by Rice (1968).

For an isotropic functionally graded material with temperature dependent thermal and mechanical properties, the elastic stress-strain relations are given by Noda (2002)

$$\sigma_{ij} = 2\mu\varepsilon_{ij} + \left[\lambda\varepsilon_{kk} - (3\lambda + 2\mu) \int_{T^*}^{T} \alpha(\xi) d\xi \right] \delta_{ij} \tag{2}$$

Where μ and λ are Lamé constants which may depend on position and temperature and α is the coefficient of thermal expansion which is also taken to be dependent on temperature and position. T is the temperature at any point and T^* is the reference stress-free temperature. δ_{ij} denotes the Kronecker delta. Also the strain energy density is given by

$$W = \frac{1}{2} \sigma_{ij} \left(\varepsilon_{ij} - \int_{T^*}^{T} \alpha(\xi) d\xi \delta_{ij} \right) \tag{3}$$

Here it is assumed that a generic material property of the constituent materials of the FGM is dependent on the temperature through the following expression

$$P = P_0 (P_{-1}/T + 1 + P_1 T + P_2 T^2 + P_3 T^3) \tag{4}$$

Where P is a material property (elasticity modulus, thermal conductivity and coefficient of thermal expansion) and P_0, P_{-1}, P_1, P_2 and P_3 are coefficients. Substituting Eq. (2) into Eq. (3) and using Eq. (4) it is possible to write

$$W = W(\varepsilon_{ij}, \mu, \lambda, \chi) \tag{5}$$

Where χ is defined as

$$\chi = \chi(x_k, T) = \int_{T^*}^{T} \alpha(\xi) d\xi \tag{6}$$

It should be noted that for the cases of plane stress and plane strain considered in this study, the strain dependency of elastic strain energy density is only upon the in-plane components of the symmetric strain tensor (i.e., ε_{11}, ε_{22}, ε_{12}).

Following the procedure given by Dag (2007), which is omitted here for brevity, in the case of crack with traction-free surfaces the J_k-integral defined in Eq. (1) on a vanishing small contour at the crack tip can be converted to a combination of area and line integrals (on the crack surface) and is given by

$$J_1 = \iint_A (\sigma_{ij} u_{i,1} - W\delta_{1j}) q_{,j} dA - \iint_A (W_{,1})_{\text{exp}\,l} q dA \tag{7}$$

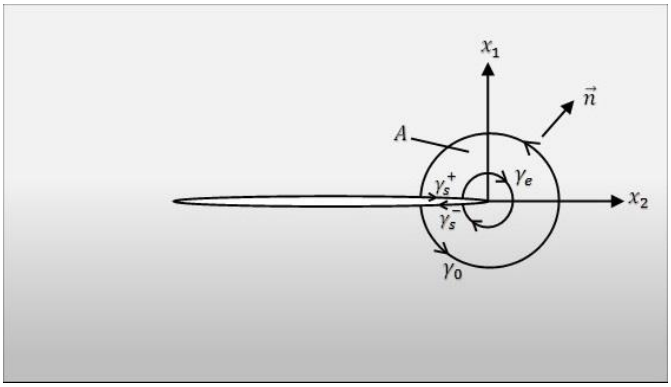

Fig. 2 A closed curve around crack tip in FGM medium

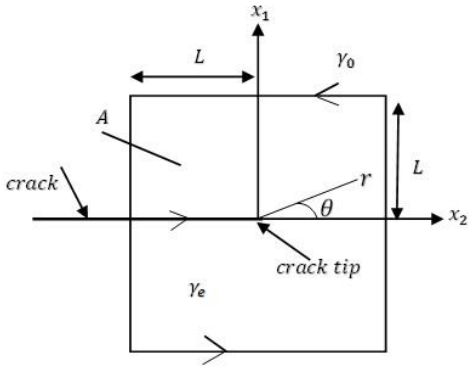

Fig. 3 A square path around crack tip

$$J_2 = \iint_A (\sigma_{ij} u_{i,2} - W\delta_{2j}) q_{,j} dA - \iint_A (W_{,2})_{\exp l} q dA - \int_{\gamma_S^-} W^- q ds - \int_{\gamma_S^+} W^+ q ds \tag{8}$$

Where i, j=1, 2 and the area A and the contours γ_s^+ and γ_s^- are shown in Fig. 2. Also W^- and W^+ represent strain energy densities evaluated on the lower and upper crack faces respectively.

Expression for $(W_{,k})_{expl}$ is given by:

$$(W_{,k})_{\exp l} = \frac{\partial W}{\partial \mu}\left(\frac{\partial \mu}{\partial T}\frac{\partial T}{\partial x_k} + \frac{\partial \mu}{\partial x_k}\right) + \frac{\partial W}{\partial \lambda}\left(\frac{\partial \lambda}{\partial T}\frac{\partial T}{\partial x_k} + \frac{\partial \lambda}{\partial x_k}\right) + \frac{\partial W}{\partial \chi}\left(\frac{\partial \chi}{\partial T}\frac{\partial T}{\partial x_k} + \frac{\partial \chi}{\partial x_k}\right) \tag{9}$$

Terms $\partial\mu/\partial T$, $\partial\lambda/\partial T$ and $\partial\chi/\partial T$ can be computed at each point by using Eq. (4). Other terms in Eq. (9) can be calculated numerically during finite element computations by using appropriate shape functions of isoparametric elements.

Considering the square path defined in Fig. 3, Eq. (8) can be rewritten as

$$J_2 = \iint_A (\sigma_{ij} u_{i,2} - W\delta_{2j}) q_{,j} dA - \iint_A (W_{,2})_{\exp l} q dA - \int_{\gamma_S} (W^+ - W^-) q ds \qquad (i, j = 1,2) \tag{10}$$

Smooth function "q" for square path can be expressed as (Dag 2007)

$$q(x_1,x_2)=\begin{cases}1-\dfrac{x_1}{L}, & -\dfrac{\pi}{4}<\theta<\dfrac{\pi}{4}\\ 1-\dfrac{x_2}{L}, & \dfrac{\pi}{4}<\theta<\dfrac{3\pi}{4}\\ 1+\dfrac{x_1}{L}, & \dfrac{3\pi}{4}<\theta<\dfrac{5\pi}{4}\\ 1+\dfrac{x_2}{L}, & \dfrac{5\pi}{4}<\theta<\dfrac{7\pi}{4}\end{cases} \tag{11}$$

2.2 Mixed-mode stress intensity factors calculation

For the purpose of mixed mode stress intensity factors calculation, the following parameter is introduced by Dag (2007)

$$\hat{J}_2=\iint_A(\sigma_{ij}u_{i,2}-W\delta_{2j})q_{,j}dA-\iint_A(W_{,2})_{\exp l}qdA-\int_0^{L-\delta}(W^+-W^-)qdx \qquad (i,j=1,2) \tag{12}$$

Where δ is the portion of path γ_s on which W is approximated by its asymptotic expression and x is the integration path variable starting from the intersection point of the path γ_0 with the crack line.

By computing this parameter for two values of δ, i.e., $\hat{J}_2^{\delta 1}$ and $\hat{J}_2^{\delta 2}$, it can easily be shown that (Dag 2007) J_2 can be expressed as

$$J_2=\frac{\sqrt{\delta_1}\left(1-\dfrac{\delta_1}{3L}\right)\hat{J}_2^{\delta_2}-\sqrt{\delta_2}\left(1-\dfrac{\delta_2}{3L}\right)\hat{J}_2^{\delta_1}}{\sqrt{\delta_1}\left(1-\dfrac{\delta_1}{3L}\right)-\sqrt{\delta_2}\left(1-\dfrac{\delta_2}{3L}\right)} \tag{13}$$

Furthermore the following relations exist between J_k-integral components and stress intensity factors

$$J_1=\frac{K_I^2+K_{II}^2}{E'_{tip}}, \quad J_2=-\frac{2K_IK_{II}}{E'_{tip}} \tag{14}$$

Where $E'_{tip}=E_{tip}$ for plane stress and $E'_{tip}=E_{tip}/(1-\nu_{tip}^2)$ for plane strain in which E_{tip} and ν_{tip} denote elasticity modulus and Poisson's ratio at the crack tip. Thus it may be concluded that

$$K_I=\pm\left\{\frac{E'J_1}{2}\left[1\pm\sqrt{1-\left(\frac{J_2}{J_1}\right)^2}\right]\right\}^{1/2} \tag{15}$$

$$K_{II}=\pm\left\{\frac{E'J_1}{2}\left[1\pm\sqrt{1-\left(\frac{J_2}{J_1}\right)^2}\right]\right\}^{1/2} \tag{16}$$

As explained by Dag (2007), the signs of the stress intensity factors and that of the term within brackets are determined by monitoring relative normal and tangential displacements near the crack tip, which are defined as (Eischen 1987, Kim and Paulino 2002)

$$\Delta_n = u_2^+ - u_2^- \qquad \Delta_t = u_1^+ - u_1^- \tag{17}$$

Where the superscripts (+) and (−) refer to the upper and lower crack surfaces, respectively. In the finite element analysis, Δ_n and Δ_t are calculated in the close vicinity of the crack tip. A positive Δ_n value implies that crack is open near the crack tip and K_I is positive. Similarly, K_{II} is positive if $\Delta_t>0$. Following conditions are used to determine the sign of the term within the brackets in Eq. (15) (Kim and Paulino 2002)

$$If \ |\Delta_n| \geq |\Delta_t| \quad take \quad [+] \tag{18}$$

$$If \ |\Delta_n| < |\Delta_t| \quad take \quad [-] \tag{19}$$

The sign of the term within the brackets in Eq. (16) has to be opposite to the sign obtained by using conditions in Eqs. (18) or (19).

3. Finite element modeling and computation

For computation of needed nodal displacement and also temperature distribution around crack tip, finite element simulations using the commercial software ABAQUS are performed. UMAT and UMATHT subroutines are used to implement variation of thermo-mechanical properties in the FE models and to assign material property of each integration point in the element due to its position and temperature. A MATLAB post-processing routine based on the J_k-integral formulation derived in previous section is developed to calculate mixed-mode SIFs from the FE analysis results. The procedure for computing mixed-mode SIFs from FE simulations and the post-processing technique based on the developed J_k-integral is schematically shown in Fig. 4.

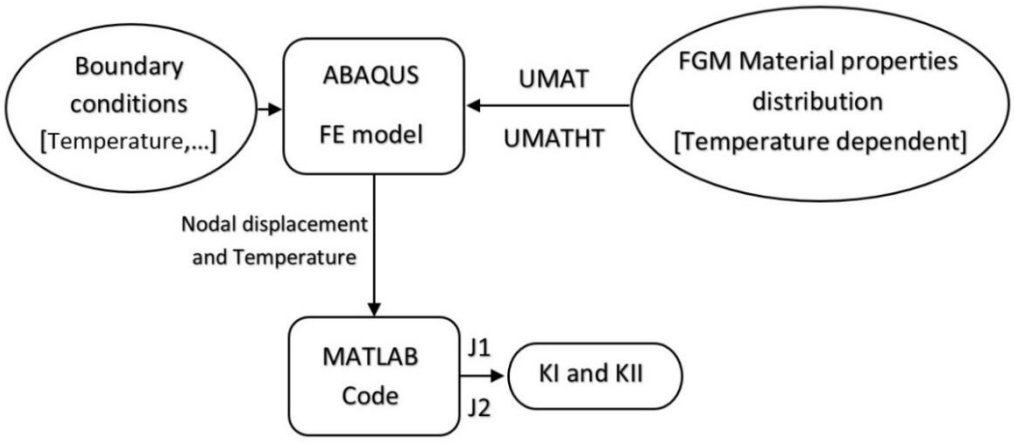

Fig. 4 Procedure of calculating stress intensity factors of a crack tip in FGM medium based on FE model

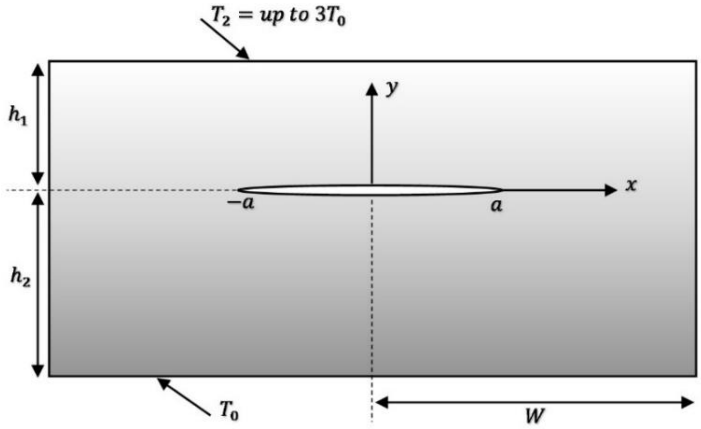

Fig. 5 Problem model geometry, an embedded crack in FGM medium

4. Numerical results

In order to investigate the effect of temperature dependent material properties on crack tip fracture parameters, problem of an embedded crack in a functionally graded material subjected to thermal stresses is considered. The same problem with temperature-independent material properties has been considered by Dag (2007) and here we investigate the effect of variation of material properties with temperature on the mixed-mode SIFs. Geometry and boundary conditions of the problem is shown in Fig. 5. The FG material is assumed to consist of Silicon Nitride-Stainless Steel, whose material properties vary continuously from Stainless Steel at y=-h_2 to Silicon Nitride at y=h_1. An embedded crack of length 2a is located at y=0 and aligned parallel to the boundaries and perpendicular to direction of material gradation. The layer is initially assumed to be kept at reference temperature of T_0 (300°K). Temperature of other surface at y=h_1 is assumed to be variable from T_0 (300°K) to 3T_0 (900°K) in 100°K increments. All other surfaces including crack faces except y=h_1 and y=-h_2 are considered to be insulated which leads to a two dimensional temperature field near crack faces.

Material property variation through FGM medium are defined by following equations

$$E(y) = E_{cr} + (E_m - E_{cr})\left(\frac{h_1 - y}{h_1 + h_2}\right)^{\gamma_1} \quad -h_2 < y < h_1 \tag{20}$$

$$\alpha(y) = \alpha_{cr} + (\alpha_m - \alpha_{cr})\left(\frac{h_1 - y}{h_1 + h_2}\right)^{\gamma_2} \quad -h_2 < y < h_1 \tag{21}$$

$$k(y) = k_{cr} + (k_m - k_{cr})\left(\frac{h_1 - y}{h_1 + h_2}\right)^{\gamma_3} \quad -h_2 < y < h_1 \tag{22}$$

Eqs. (20)-(22) defines variation of modulus of elasticity, coefficient of thermal expansion and

Table 1 Coefficients of Eq. (4) for $E(T)$, $\alpha(T)$ and $k(T)$ obtained from experimental data by Touloukian (1967)

Material		P_0	P_{-1}	P_1	P_2	P_3
Silicon Nitride	$E_{cr}(T)$	348.43×10^{9}	0	-3.07×10^{-4}	2.160×10^{-7}	-8.946×10^{-11}
	$\alpha_{cr}(T)$	5.8723×10^{-6}	0	9.095×10^{-4}	0	0
	$k_{cr}(T)$	13.723	0	-1.032×10^{-3}	5.466×10^{-7}	-7.876×10^{-11}
Stainless Steel	$E_m(T)$	201.04×10^{9}	0	3.079×10^{-4}	-6.534×10^{-7}	0
	$\alpha_m(T)$	12.330×10^{-6}	0	8.086×10^{-4}	0	0
	$K_m(T)$	15.379	0	-1.264×10^{-3}	2.092×10^{-6}	-7.223×10^{-10}

thermal conductivity through *y* direction. Subscripts "*cr*" denotes for ceramic material properties and "*m*" denotes for metallic material properties. Exponents γ_1, γ_2 and γ_3 are positive constants.

Material properties dependency on temperature is defined by Eq. (4). Coefficients of Eq. (4) for modulus of elasticity, coefficient of thermal expansion and conductivity can be determined from experimental data available in the book by Touloukian (1967) and also reported by Reddy and Chin (1998). Numerical values of these coefficients for silicon nitride and stainless steel obtained from experimental data are given in Table 1.

By using Eq. (4) each material property can be compensated with temperature variation; and then Eqs. (20)-(22) are used for computing material variation in FGM medium.

Steady state temperature distribution in the FG layer can be determined by solving the following nonlinear differential equation for the one-dimensional governing heat transfer equation

$$\frac{d}{dy}\left[k(y,T)\frac{dT}{dy}\right]=0 \tag{23}$$

Subjected to the following boundary conditions

$$T(-h_2)=T_0 \qquad T(h_1)=T_2 \tag{24}$$

Eq. (23) is a nonlinear differential equation in which the conductivity coefficient is dependent upon both the temperature distribution and the spatial coordinates. This equation should be solved using iterative methods. In this study the temperature distribution is determined by implementing the spatial and temperature dependent conductivity coefficient in the FE model employing user subroutine UMATHT. The temperature distribution is then calculated by performing a heat transfer analysis in the FE module.

For the cracked FG problem shown in Fig. 5, *x*-direction displacements are anti-symmetric and *y*-direction displacements are symmetric about *y*-axis. Thus it is sufficient to model half of the layer and analyze only one of the crack tips. In this study the region $0<x<W$ is considered and modeled for calculation of crack tip fracture parameters at $x=a$. It should be noted that mixed mode stress intensity factors of the crack tip at $x=-a$ have the following relation with mixed mode stress intensity factors of the crack tip at $x=a$

$$K_I(-a)=K_I(a) \qquad and \qquad K_{II}(-a)=-K_{II}(a) \tag{25}$$

To investigate the influence of variation in thermal conductivity on steady state temperature distribution in material through crack surfaces, the thermal conductivity is considered to be once

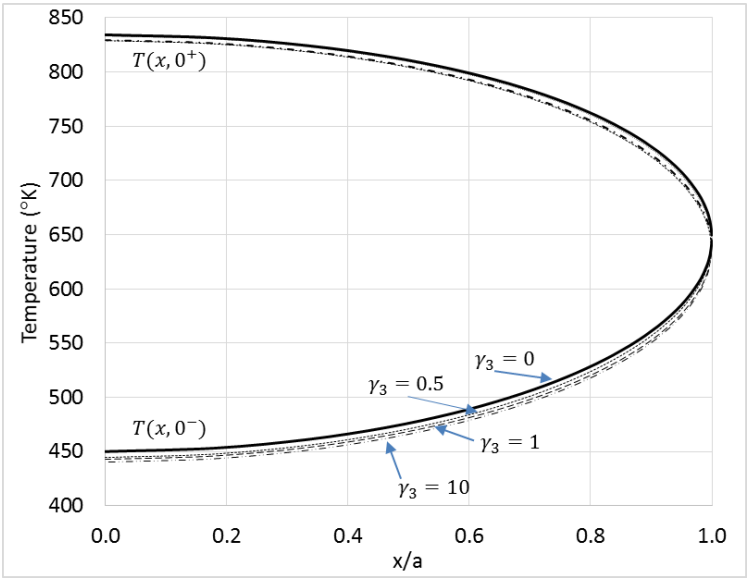

Fig. 6 Temperature profiles of crack surfaces for various values of γ_3 and temperature independent thermal conductivity

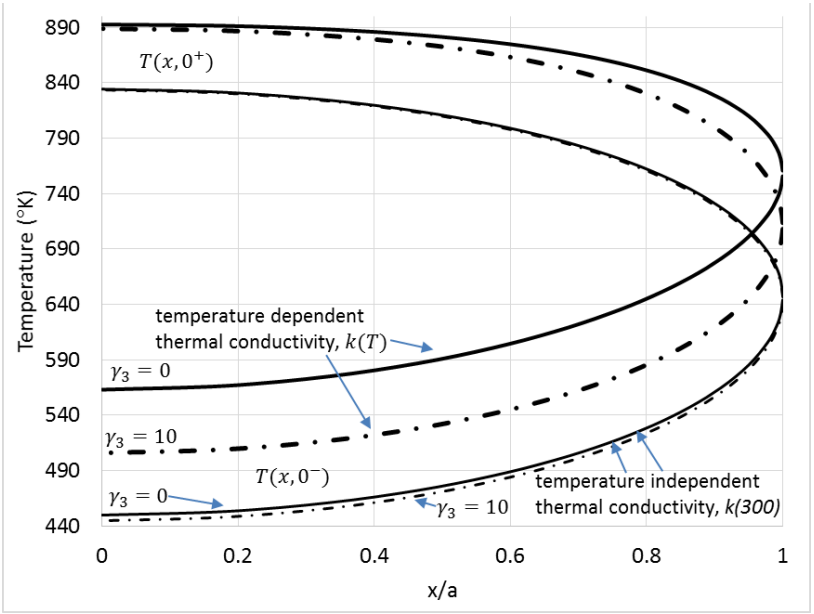

Fig. 7 Temperature profiles of crack surfaces. A comparison between result for thermal conductivity dependent on temperature and independent of temperature change

temperature independent and then temperature dependent and the results of temperature distribution corresponding to these two cases are compared.

Fig. 6 illustrates the steady state temperature distribution on crack surfaces for various values of exponent γ_3 while ceramic (silicon nitride) and metal (stainless steel) thermal conductivities are

set to k_{cr} (300°K) and k_m (300°K) and independent of temperature change. Since no heat flow is assumed on the crack faces, temperature of the upper and lower crack surfaces are not equal.

$T(x, 0^+)$ represents temperatures of upper surface of the cracks and a point on this surface has larger temperature than the corresponding temperature of the point on the lower crack surface which is indicated by $T(x, 0^-)$. These two temperature profiles merge at $x \to a$. Also it can be seen that as γ_3 increases (shift from metal rich FGM to ceramic rich material) temperature values decrease.

In Fig. 7 temperature profiles of crack surfaces for various FG exponents are shown and effect of the temperature-dependency of thermal conductivity of FG material on the temperature distribution of the crack faces is also shown in this figure. These temperature profiles with thermal conductivity independent and dependent to temperature for two values of exponent γ_3 are compared. Temperature profiles have higher values when thermal conductivity considered temperature variable and also values of exponent γ_3 has more distinct impact on temperature profile in this case in compare to thermal conductivity to be considered temperature independent. Temperature profile of lower surface of the crack $T(x, 0^-)$ shows more variation in temperature level with different exponent γ_3 values, but upper surface of the crack tend to have same temperature level with different exponent γ_3. It stems from the fact that thermal conductivity variation of the metals (stainless steel) by temperature change is much higher than ceramic part (silicon nitride).

Fig. 8 shows the deformation of the FG layer under the applied thermal loading and the two-dimensional temperature distribution. The states of elements in the crack tip region for the un-deformed and deformed configurations are also indicated in this figure.

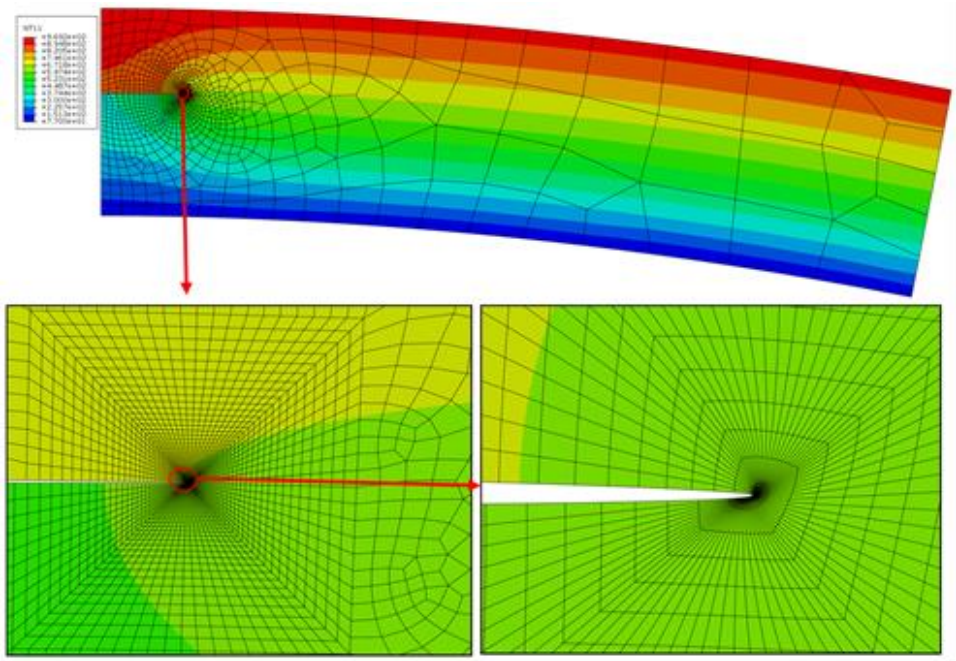

Fig. 8 Temperature distribution in the deformed configuration of the FG layer (up), and the crack front region mesh for the un-deformed and deformed configurations (down).

Table 2 Normalized mixed mode stress intensity factors with temperature independent material properties computed by Dag (2007), enriched finite elements (EFE) and by this study. h_1/a=0.5, h_2/a=2, W/a=10, γ_1=1.5, γ_3=2, $K_{In}=K_I(a)/K_0$, $K_{IIn}=K_{II}(a)/K_0$, $K_0=\sigma_0\sqrt{(\pi a)}$, $\sigma_0=E_{cr}\alpha_{cr}T_0$

			J_k-integral by Dag (2007)	EFE*	J_k-integral, this study
Plane Strain	γ_2 = 0.5	K_{In}	0.0500	0.0502	0.0501
		K_{IIn}	0.1314	0.1312	0.1314
	γ_2 = 2	K_{In}	0.0403	0.0405	0.0402
		K_{IIn}	0.1063	0.1064	0.1061

*(Dag *et al*. 2004, Yildirim and Erdogan 2004)

In order to verify our results for SIF computation, mixed-mode thermal SIF results obtained from present analysis are compared to those reported by Dag (2007) using the same J_k-integral approach and also to the results reported in (Dag *et al.* 2004, Yildirim and Erdogan 2004) which are computed using extended finite element method in Table 2. The material properties are assumed to be temperature independent. Good agreement between the results of current study with those reported in the mentioned references is observed.

In the following it is assumed that the material properties vary according to the same FG index parameter, i.e., $\gamma_1=\gamma_2=\gamma_3=\gamma$. In order to investigate effect of temperature dependent material properties on crack tip fracture parameters, the temperature gradient between two surfaces of the model is varied and effect of each material gradation index under conditions of temperature variable material properties and temperature independent material properties on the SIFs are presented. In Fig. 9(a) and Fig. 9(b), mode one (K_I) and mode two (K_{II}) stress intensity factors as a function on temperature gradient between two surfaces of the model for both temperature dependent material properties (TDMP) and temperature independent material properties (TIMP)

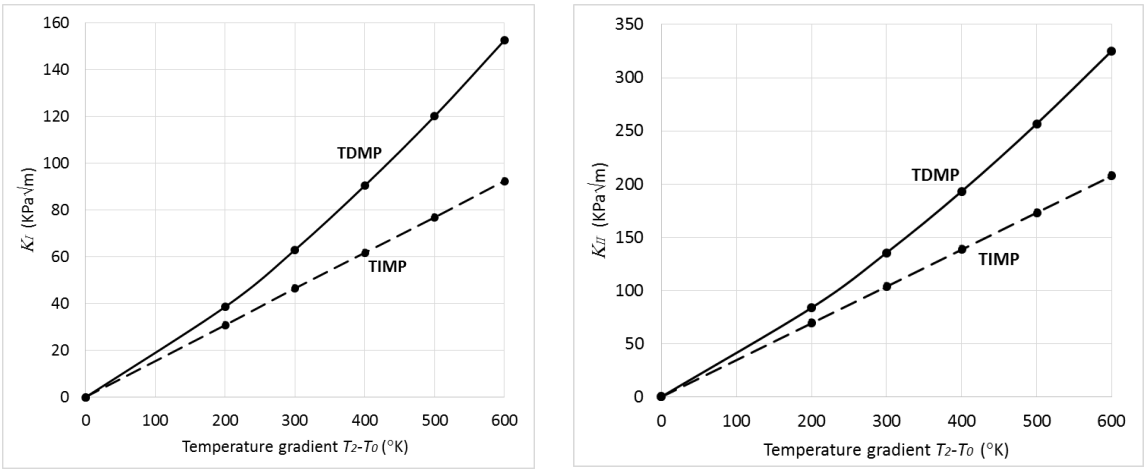

(a) Mode one stress intensity factor (K_I) (b) Mode two stress intensity factor (K_{II})

Fig. 9 Stress Intensity Factors (SIF) as a function of temperature gradient on model, in two states of temperature dependent material properties (TDMP) and temperature independent material properties (TIMP), γ = 2, T_0 =300°K

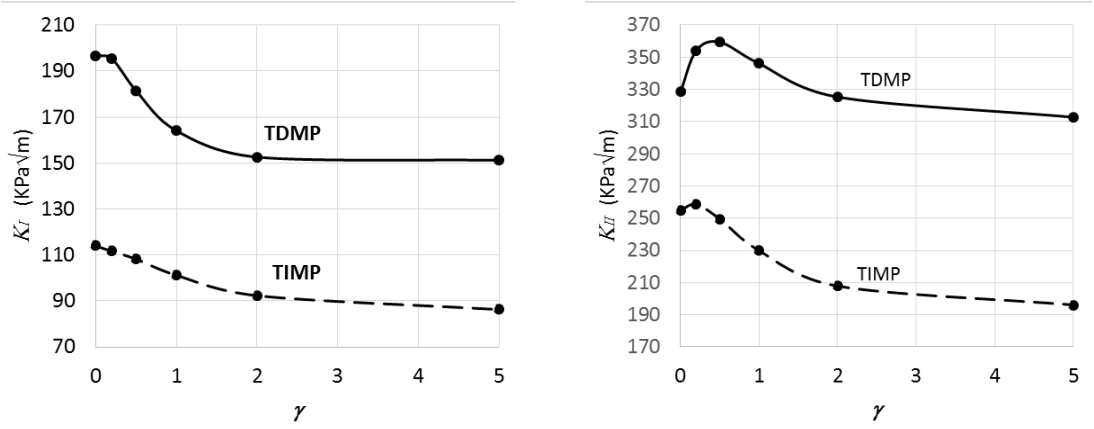

(a) Mode one stress intensity factor (K_I) (b) Mode two stress intensity factor (K_{II})

Fig. 10 Stress intensity factors (SIFs) as a function of γ, in two states of TDMP and TIMP. T_2 = 900°K

Table 3 Mixed mode stress intensity factors for various values of γ at two different T_2 values in two states of material properties. TD: temperature dependent material properties and TI: temperature independent material properties. $\gamma_1 = \gamma_2 = \gamma_3 = \gamma$.

γ	J_k-integral	T_0=300°K, T_2=600°K ΔT=300°K				T_0=300°K, T_2=900°K ΔT=600°K			
	$KPa\sqrt{m}$	K_{TI}	K_{TD}	ΔK	$\Delta K/K_{TD}$	K_{TI}	K_{TD}	ΔK	$\Delta K/K_{TD}$
0	K_I	57.09	81.93	24.85	%30.3	114.18	196.65	82.47	%41.9
	K_{II}	127.36	156.96	29.60	%18.9	254.71	328.68	73.97	%22.5
0.2	K_I	55.93	78.30	22.37	%28.6	111.71	195.38	83.67	%42.8
	K_{II}	129.28	161.04	31.76	%19.7	258.61	354.15	95.54	%27.0
0.5	K_I	54.10	73.75	19.66	%26.7	108.36	181.42	73.06	%40.3
	K_{II}	124.8	157.23	32.43	%20.6	249.53	359.36	109.83	%30.6
1	K_I	50.98	68.41	17.43	%25.5	101.30	164.07	62.77	%38.3
	K_{II}	114.82	146.97	32.15	%21.9	229.92	346.08	116.16	%33.6
2	K_I	46.43	63.03	16.61	%26.4	92.39	152.61	60.23	%39.5
	K_{II}	103.83	135.44	31.61	%23.3	207.87	325.29	117.42	%36.1
5	K_I	43.07	60.79	17.72	%29.2	86.30	151.20	64.90	%42.9
	K_{II}	98.10	129.16	31.06	%24.1	196.11	312.77	116.66	%37.3
10	K_I	43.41	61.14	17.72	%29.0	86.05	151.91	65.86	%43.4
	K_{II}	96.97	128.1	31.13	%24.3	194.30	310.92	116.62	%37.5
20	K_I	43.63	61.03	17.39	%28.5	86.58	152.32	65.75	%43.2
	K_{II}	96.55	127.86	31.31	%24.5	193.39	310.21	116.82	%37.7

are illustrated, respectively. From these figures it can be concluded that in temperature variable material properties state, mixed mode stress intensity factor changes are linear with temperature gradient while when material properties considered temperature variable, these crack tip parameters change non-linear. Also in TDMP state, K_I and K_{II} are higher and also as T_2 increases,

difference between TDMP and TIMP stress intensity factors became higher.

In Fig. 10(a) and Fig. 10(b), mode one and mode two stress intensity factors (K_I and K_{II}) for the two cases of TDMP and TIMP are illustrated as a function of γ when T_2=900°K. From these figures it may be concluded that mixed mode stress intensity factors for the case of TDMP are higher than the SIFs for the case of TIMP, and SIFs corresponding to FGM indices with $0<\gamma<1$ are more critical than those corresponding to $1<\gamma$.

In Table 3 mixed mode stress intensity factors for two cases of TIMP and TDMP for two values of upper surface temperature T_2=600°K and T_2=900°K and various values of FGM index γ are presented. Also in this table the amount of difference between each mixed mode stress intensity factors calculated when material properties are temperature dependent and temperature independent are given. Results in Table 3 show that mixed mode stress intensity factors calculated with TDMP are always higher than when SIFs are calculated with TIMP. Furthermore, increase in temperature gradient ($\Delta T=T_2-T_0$) leads in more difference between crack tip parameters calculated with TIMP and TDMP assumptions. Finally the percentage of difference between two values ($\Delta K/K_{TD}$) increases as the FGM index γ decreases.

5. Conclusions

In this study, effects of temperature dependent material properties on mixed mode facture analysis of functionally graded materials under thermal loading was investigated. Mixed mode stress intensity factors obtained from a domain form of J_k-integral including thermal effects and temperature dependent material properties were calculated. The modified form of J_k-integral was implemented in a post-processing routine to compute mixed-mode fracture parameters of FGMs from the displacement field obtained from FE analysis. Verification examples showed the accuracy of the adopted technique in computation of mixed-mode thermal SIFs. Results of mixed-mode thermal SIFs for an illustrative example were provided for cases of temperature independent and temperature dependent material properties and the following conclusions are drawn:

- Temperature profiles of crack surfaces around crack tip have higher values when thermal conductivity of the material is considered to be variable with temperature.
- Mixed mode stress intensity factors calculated with considering temperature dependent material properties are higher than the corresponding mixed-mode SIFs when the temperature dependency is not considered. This difference is up to 43% for mode two stress intensity factors and 38% for mode one stress intensity factors.
- The difference between the SIF results obtained from considering two cases of temperature dependent and temperature independent material properties increases with the magnitude of applied temperature boundary condition.

Results of current study reveal that for accurate determination of thermal SIFs in cracked functionally graded materials, it is essential to consider the variation of thermo-mechanical properties with temperature in their fracture analysis especially when high temperature profiles are present in the material.

References

Abolbashari, M.H. and Nazari, F. (2014), "A multi-crack effects analysis and crack identification in

functionally graded beams using particle swarm optimization algorithm and artificial neural network", *Struct. Eng. Mech.*, **51**(2), 299-313.
Atkinson, C. and List, R. (1978), "Steady state crack propagation into media with spatially varying elastic properties", *Int. J. Eng. Sci.*, **16**(10), 717-730.
Bhardwaj, G., Singh, I., Mishra, B. and Bui, T. (2015), "Numerical simulation of functionally graded cracked plates using NURBS based XIGA under different loads and boundary conditions", *Compos. Struct.*, **126**, 347-359.
Birman, V. and Byrd, L.W. (2007), "Modeling and analysis of functionally graded materials and structures", *Appl. Mech. Rev.*, **60**(5), 195-216.
Dag, S. (2007), "Mixed-mode fracture analysis of functionally graded materials under thermal stresses: a new approach using J_k-integral", *J. Therm. Stress.*, **30**(3), 269-296.
Dag, S., Yildirim, B. and Erdogan, F. (2004), "Interface crack problems in graded orthotropic media: Analytical and computational approaches", *Int. J. Fract.*, **130**(1), 471-496.
Delale, F. and Erdogan, F. (1983), "The crack problem for a nonhomogeneous plane", *J. Appl. Mech.*, **50**(3), 609-614.
Eischen, J. (1987), "An improved method for computing the J2 integral", *Eng. Fract. Mech.*, **26**(5), 691-700.
Eshraghi, I. and Soltani, N. (2015), "Stress intensity factor calculation for internal circumferential cracks in functionally graded cylinders using the weight function approach", *Eng. Fract. Mech.*, **134**, 1-19.
Gu, P., Dao, M. and Asaro, R. (1999), "A simplified method for calculating the crack-tip field of functionally graded materials using the domain integral", *J. Appl. Mech.*, **66**(1), 101-108.
Guo, L.C. and Noda, N. (2007), "Modeling method for a crack problem of functionally graded materials with arbitrary properties-piecewise-exponential model", *Int. J. Solid. Struct.*, **44**(21), 6768-6790.
Kim, J.H. and Paulino, G.H. (2002), "Mixed-mode fracture of orthotropic functionally graded materials using finite elements and the modified crack closure method", *Eng. Fract. Mech.*, **69**(14), 1557-1586.
Kim, J.H. and Paulino, G.H. (2002), "Finite element evaluation of mixed mode stress intensity factors in functionally graded materials", *Int. J. Numer. Meth. Eng.*, **53**(8), 1903-1935.
Koizumi, M. (1997), "FGM activities in Japan", *Compos. Part B: Eng.*, **28**(1), 1-4.
Noda, N. (1991), "Thermal stresses in materials with temperature-dependent properties", *Appl. Mech. Rev.*, **44**(9), 383-397.
Noda, N. (2002), *Thermal Stresses*, CRC Press, New York, NY, USA.
Ootao, Y. and Ishihara, M. (2013), "Asymmetric transient thermal stress of a functionally graded hollow cylinder with piecewise power law", *Struct. Eng. Mech.*, **47**(3), 421-442.
Petrova, V. and Sadowski, T. (2014), "Theoretical modeling and analysis of thermal fracture of semi-infinite functionally graded materials with edge cracks", *Meccanica*, **49**(11), 2603-2615.
Reddy, J. (2000), "Analysis of functionally graded plates", *Int. J. Numer. Meth. Eng.*, **47**(1-3), 663-684.
Reddy, J. and Chin, C. (1998), "Thermomechanical analysis of functionally graded cylinders and plates", *J. Therm. Stress.*, **21**(6), 593-626.
Rice, J.R. (1968), "A path independent integral and the approximate analysis of strain concentration by notches and cracks", *J. Appl. Mech.*, **35**(2), 379-386.
Sumi, N. and Sugano, Y. (1997), "Thermally induced stress waves in functionally graded materials with temperature-dependent material properties", *J. Therm. Stress.*, **20**(3-4), 281-294.
Touloukian, Y. S., (1967), *Thermophysical Properties of High Temperature Solid Materials*, Macmillan, London, England.
Yildirim, B. and Erdogan, F. (2004), "Edge crack problems in homogenous and functionally graded material thermal barrier coatings under uniform thermal loading", *J. Therm. Stress.*, **27**(4), 311-329.
Yu, H. and Kitamura, T. (2015), "A new domain-independent interaction integral for solving the stress intensity factors of the materials with complex thermo-mechanical interfaces", *Eur. J. Mech. A/Solid.*, **49**, 500-509.